# Bulk and surface electronic structure of hexagonal boron nitride

A. Catellani,* M. Posternak, and A. Baldereschi†
*Institut de Physique Appliquée, Ecole Polytechnique Fédérale, CH-1015 Lausanne, Switzerland*

A. J. Freeman
*Department of Physics and Astronomy, Northwestern University, Evanston, Illinois 60201*
(Received 23 April 1987)

Accurate full-potential self-consistent linearized augmented-plane-wave (FLAPW) calculations have been carried out for hexagonal boron nitride. The resulting energy-band structure indicates that this material is an indirect-gap insulator and shows the existence of two unoccupied interlayer bands, similar to those found in graphite and graphite intercalation compounds. Chemical bonding is mainly covalent, with a small charge transfer towards the nitrogen atoms. Moreover, model-potential calculations, based on first-principles FLAPW wave functions and potentials, have been used to study slabs of thickness up to 35 layers. Contrary to the case of graphite, our results do not provide evidence of surface states associated with the interlayer bands.

## I. INTRODUCTION

Hexagonal boron nitride (*h*-BN) is an interesting quasi-two-dimensional insulating analog to semimetallic graphite. The properties of this material, which has recently gained considerable importance in the GaAs semiconductor industry, have been studied extensively both experimentally and theoretically,[1] but agreement has not yet been achieved on basic electronic properties such as the value of the lowest excitation energies.

Electronic states have been studied experimentally by optical absorption,[2–5] reflectivity,[6,7] x-ray photoemission spectroscopy (XPS) measurements,[8,9] electron energy loss spectroscopy (EELS),[10–12] and other techniques.[13,14] All absorption studies concluded that *h*-BN is a direct-gap insulator; they disagree, however, in the value of the lowest band gap which ranges between 3.8 eV (Ref. 5) and 5.8 eV (Refs. 3 and 4). This large discrepancy has been attributed to the different quality of the samples used, as it is difficult to grow good single crystals of this material. In fact, the absorption spectrum of *h*-BN shows in the range 1–5 eV a broad continuum whose extrinsic and/or intrinsic nature is still controversial. The most recent optical-reflectivity study[7] indicates a direct-gap nature of *h*-BN with an energy gap of 5.2 eV. The values of the band gap measured by EELS range between 5.0 eV (Ref. 11) and 5.7 eV (Ref. 12).

Energy bands have been calculated in both the two-dimensional approximation using the semiempirical[15–17] and self-consistent linear combination of atomic orbitals[18] (LCAO) method, and for the real three-dimensional crystal with the LCAO (Refs. 4, 19, and 20) and the orthogonalized-plane-wave[21] (OPW) method. All these theoretical studies conclude that *h*-BN is a direct-gap insulator, provide a valence-band dispersion which is in general agreement with the experimental data, and give band-gap values between 2.45 (Ref. 14) and 12.7 eV (Ref. 18). Precise fully converged self-consistent calculations have not been reported for this material.

In a recent preliminary report[22] we have shown that a simple LCAO approach with a minimal basis set does not provide the correct band structure of *h*-BN above the Fermi level. In particular, when a set of basis functions with sufficient variational freedom is used, an additional unoccupied band appears, which exhibits free-electron-like character parallel to the atomic planes. These interlayer states are similar to those previously predicted for graphite and $LiC_6$ (Ref. 23) and whose existence has been confirmed by inverse photoemission spectroscopy.[24]

The purpose of the present paper is to present the results of a highly precise fully converged self-consistent calculation of the *h*-BN energy bands, and to discuss in detail the lowest electronic excitation energies and the nature of the interlayer states. Moreover, we will study the possible existence in *h*-BN of surface states associated with the bulk interlayer band. Such states in fact exist in graphite, as has been shown both theoretically[25] and experimentally.[24]

## II. METHOD OF CALCULATION

Hexagonal BN has $D_{6h}$ symmetry; its unit cell contains two formula units and extends over two consecutive layers. The experimental values of the lattice parameters at equilibrium are $a_0 = 2.504$ and $c_0 = 6.66$ Å,[26] which are very close to those of graphite.

Electronic energies and wave functions of three-dimensional *h*-BN have been calculated with the self-consistent full-potential linearized augmented-plane-wave (FLAPW) method.[27] The local-density approximation (LDA) to density-functional theory with the Hedin-Lundqvist exchange-correlation potential is used. We choose the same atomic sphere radius for both boron and nitrogen; its value, 0.688 Å (1.3 a.u.), corresponds to nearly touching spheres. In the interstitial region, the wave functions are expanded in terms of plane waves with wave vectors less than 7.56 $Å^{-1}$, and in terms of products of radial functions and spherical harmonics

 

with $l \leq 8$ inside the spheres. The electron charge density and the crystal potential are similarly expanded in terms of 2507 plane waves, and spherical harmonics with $l \leq 6$. Integrations in $k$ space were performed with the analytic tetrahedron method, using 20 points in the irreducible wedge of the Brillouin zone.

Fully converged FLAPW calculations have also been performed for values of the $c$ parameter larger than $c_0$ and up to $c = 1.75c_0$. These calculations are necessary for understanding the nature of the interlayer interaction and for investigating the possible existence of surface states.

## III. BULK ENERGY BANDS

The energy-band structure calculated at the equilibrium lattice parameters, shown in Fig. 1, yields a valence-band dispersion in close agreement with all previously reported results (see, e.g., Ref. 19). However, we predict that $h$-BN is an indirect-gap insulator and we find two additional conduction bands not yet reported in the literature for this material.

The lowest-energy band gap occurs between the valence-band maximum at $H$ and the conduction-band minimum at $M$. The value of this gap is 3.9 eV, while the lowest direct band gap ($H$ point) is 4.3 eV. This result is the first theoretical prediction of the indirect-gap nature of $h$-BN, and differs from all previous calculations in the structure of the conduction bands. This is not surprising since in our precise calculation we use throughout the Brillouin zone an average basis set of 250 augmented plane waves, which is to be compared with the basis set of 73 orthogonalized plane waves in the calculation of Nakhmanson and Smirnov,[21] or with the minimal basis set of 16 atomic orbitals used by Robertson.[19] A large basis set is a necessary condition for an accurate description of the $h$-BN energy band dispersion, and in particular that of the conduction bands. Indeed, Nakhmanson and Smirnov mention in their paper that the lowest direct gap increases from 2.45 to 3.80 eV when they expand the basis set from 73 to 150 OPW's. Besides being far from convergence, all previous calculations are also non-self-consistent. Therefore, they cannot be trusted for the description of differences in band energies of the order of 0.1 eV, such as the difference between the lowest direct and indirect energy gaps which, according to our converged self-consistent results, is 0.4 eV. We also stress that the predicted indirect-gap character of $h$-BN is compatible with all existing experimental data. Indeed, as mentioned in the Introduction, experimental spectra display a continuum of intense electronic excitations already starting at about 1 eV, and extending up to the onset of the strong intrinsic interband $\pi \rightarrow \pi$ excitations ($\sim 5$ eV). The spectral features of these electronic excitations, which probably have extrinsic origin, are strong enough to hide intrinsic indirect transitions occurring at the same energy.

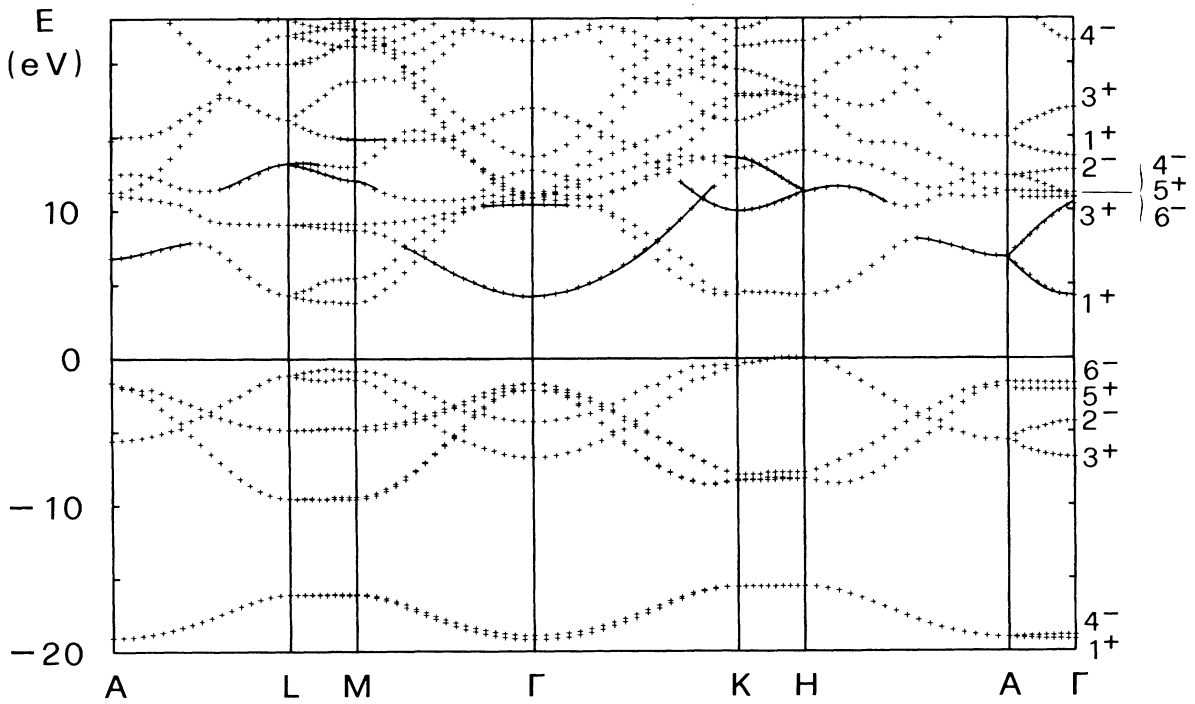


FIG. 1. Energy-band structure of hexagonal BN. Electron states at the zone center are classified following the notation used by Robertson (Ref. 19). Solid lines serve to identify the interlayer bands, which show several (anti)crossings with $\sigma$ and $\pi$ bands. The zero of energy is taken as the top of the valence band (point $H$ of the Brillouin zone). The minimum of the conduction band occurs at $M$.

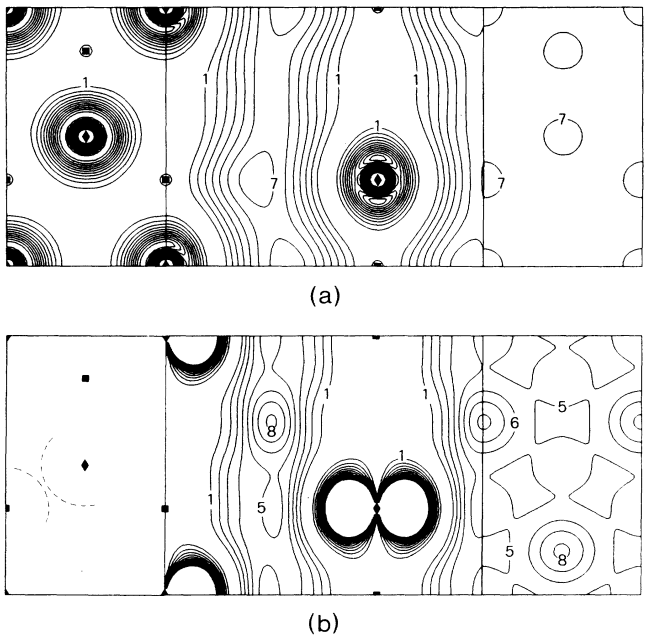


FIG. 2. Charge-density contour plot for the symmetric $\Gamma_1^+$ (a) and the antisymmetric $\Gamma_3^+$ interlayer states (b). The charge densities are displayed in the basal atomic plane (left-hand panel), in the vertical plane through a B—N bond (central panel), and in the horizontal plane bisecting the interlayer space (right-hand panel). Contour values are given in units of 0.01 $e/\text{Å}^3$, with subsequent contours separated by 0.01 $e/\text{Å}^3$. Diamonds and squares indicate nitrogen and boron sites, respectively. The dotted lines in the left panel of (b) indicate the augmented plane-wave (APW) spheres used in this work.

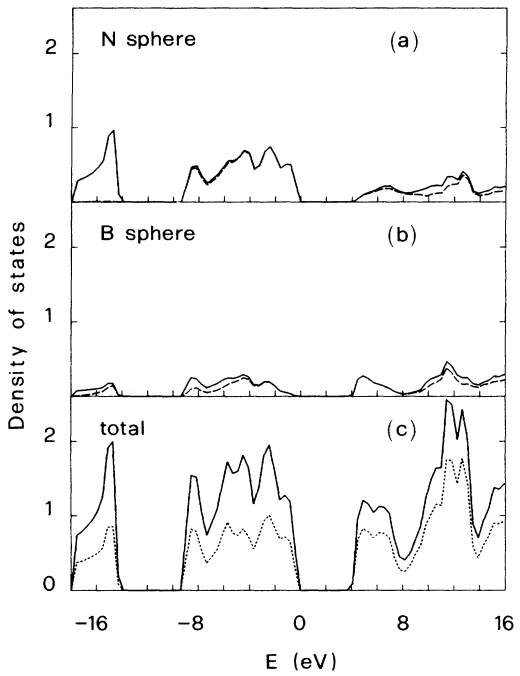


FIG. 3. Partial [(a) and (b)] and total (c) densities of states (DOS's) in the valence bands and in the low-energy conduction bands (in units of electrons/cell eV). The partial densities are the projected density of states by atom type in the corresponding APW spheres. The broken lines in (a) and (b) represent the contribution of $p$-like states to the DOS inside the spheres; the dotted line in (c) indicates the large contribution from the interstitial region in the total DOS.

The first additional empty band is the lowest unoccupied state at $\Gamma$ and presents the characteristics of an interlayer band. Indeed, as is clear from Fig. 1, this interlayer band has a strong parabolic behavior around its minimum at $\Gamma$, which is located at 4.7 eV above the top of the valence band at $H$, and is even under reflection with respect to the atomic planes. According to the notation of Robertson,[19] this state belongs to the $\Gamma_1^+$ representation. Since the unit cell contains two formula units, this band folds back at the upper hexagonal face of the Brillouin zone and gives rise to a second interlayer band at higher energy. The higher interlayer state at $\Gamma$ (10.0 eV above the valence-band top) is odd with respect to the reflection operation and has $\Gamma_3^+$ symmetry. The interlayer character of these $\Gamma$ states is clearly evident in the single-state charge-density plots of Fig. 2. The structures close to the N nuclei are the results of the effects of orthogonalization to the occupied states. These plots indicate that most of the charge is situated in the interstitial region (the calculated values are 86% and 67% for the $\Gamma_1^+$ and $\Gamma_3^+$ states, respectively). The charge distributions presented in Fig. 2 are similar to those of the interlayer states in graphite,[23] apart from a weaker interlayer character (the calculated values in graphite are 92% and 74% for the $\Gamma_1^+$ and $\Gamma_3^+$ states, respectively). Apparently, the reason why interlayer states have not been reported earlier for $h$-BN is the use of insufficient basis sets of atomic orbitals in all previous calculations.

Comparison of our results with optical data indicates that the use of LDA underestimates the lowest energy gaps by $\sim 1$ eV. We may then draw the following conclusions for the optical properties of $h$-BN near the fundamental threshold: (i) in the intrinsic material, absorption starts at $\sim 5$ eV with indirect transitions from $H$ to $M$; (ii) the lowest direct threshold occurs at the $H$ point

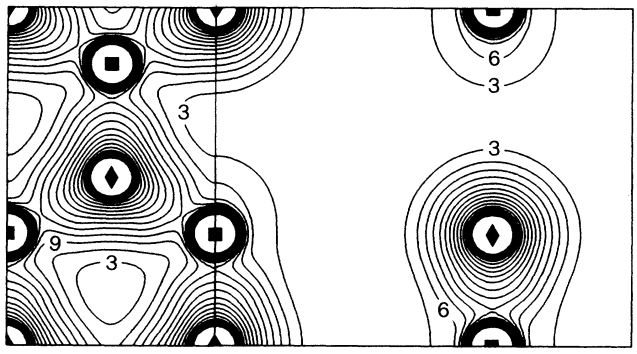

FIG. 4. Contour plots of the total electronic charge density in the basal atomic plane (left panel), and in the vertical plane through a B—N bond (right panel). Contour values are given in units of 0.1 $e/\text{Å}^3$. Subsequent contours differ by 0.3 $e/\text{Å}^3$. Atomic symbols are the same as in Fig. 2.

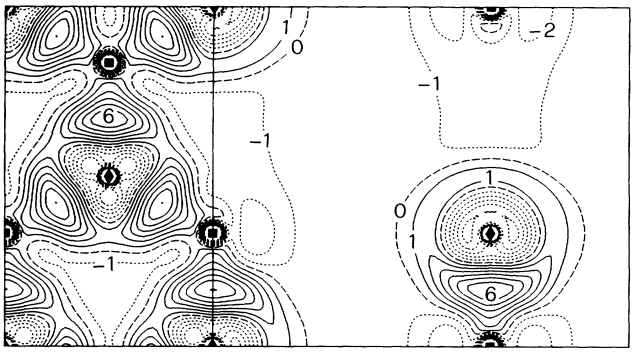


FIG. 5. Contour plots, in the same planes as those of Fig. 4, of the differential electronic charge density, i.e., the difference between the self-consistent crystal density and the superposition of self-consistent atomic densities. Contour values are given in units of 0.1 $e/\text{Å}^3$ and subsequent contours are separated by 0.1 $e/\text{Å}^3$. The broken lines indicate the zero contours, while positive (negative) contours are represented by solid (dotted) lines. Atomic symbols are the same as in Fig. 2.

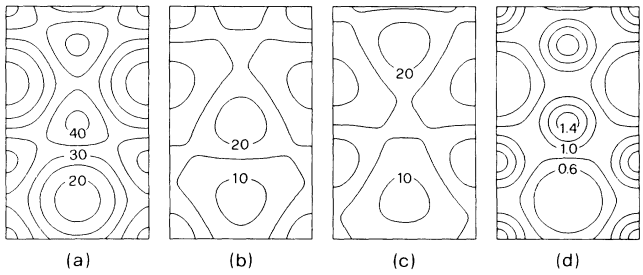


FIG. 7. (a) Contour plot of the self-consistent charge density for the crystal with $c=c_0$ in a horizontal plane bisecting the interlayer space. (b) Contour plot of the self-consistent charge density for the crystal with $c=1.75c_0$ in a horizontal plane whose distance from the atomic plane is $d=c_0/4$. (c) Same as (b), but at a distance $d=(c/2-c_0/4)$. (d) Contour plot of the polarization charge density, i.e., the difference between the charge density in (a) and the superposition of the densities in (b) and (c). Contour values are given in units of 0.001 $e/\text{Å}^3$. Subsequent contours are separated by 0.005 $e/\text{Å}^3$ in (a), (b), and (c), and by 0.0002 $e/\text{Å}^3$ in (d).

at a photon energy of $\sim 5.5$ eV; (iii) the E⊥c spectrum is dominated by a doublet near 6.5 eV, corresponding to direct transitions close to the *L*-*M* axis. Indeed, the calculated LDA bands close to *M* show the existence of two saddle points in the joint density of states at 5.4 and 5.8 eV.

Finally, in Fig. 3, we present a plot of the density of states of the valence bands and low-lying conduction bands. The calculated valence-band width (18.5 eV) is smaller than the value (20.7±1.5 eV) obtained by Tegeler *et al.*[9] in their most recent XPS measurements. According to these authors, however, the real total width of the valence bands may be smaller than the measured value by 1–3 eV, due to significant Auger broadening of the XPS spectrum at energies corresponding to the lowest valence band. The large *p*-like contribution in the lowest valence bands and in the boron sphere is an artifact resulting from our choice of atomic spheres (see Fig. 2 for sphere geometry). The lowest valence bands in fact are dominated by nitrogen 2*s* orbitals, for which the expectation value of the orbital radius is 1.32 a.u. Therefore, the nitrogen 2*s* orbitals extend significantly outside their sphere (with radius 1.3 a.u.) into the boron sphere, thus giving rise to an apparent boron *p*-like character.

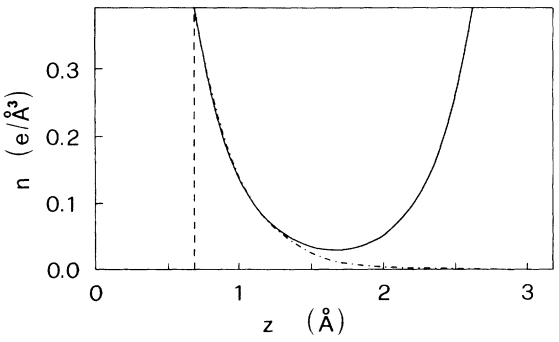


FIG. 6. Planar average of the self-consistent electronic density for the crystal with $c=c_0$ (solid line), and for the expanded crystal with $c=1.75c_0$ (long-dashed–short-dashed line). The averages are done in planes parallel to the atomic layers, and *z* measures the distance from the basal plane. The vertical broken line indicates the radius of the APW spheres.

## IV. CHEMICAL BONDING

The total valence electron density for *h*-BN is given in Fig. 4 in the basal plane and in a vertical plane containing a BN bond. Figure 5 gives the differential charge density, i.e., the difference between the self-consistent FLAPW charge density of the crystal and the superposition of self-consistent atomic charge densities centered at the lattice sites. Inspection of the two figures shows that in *h*-BN the in-plane chemical bond is mainly covalent.

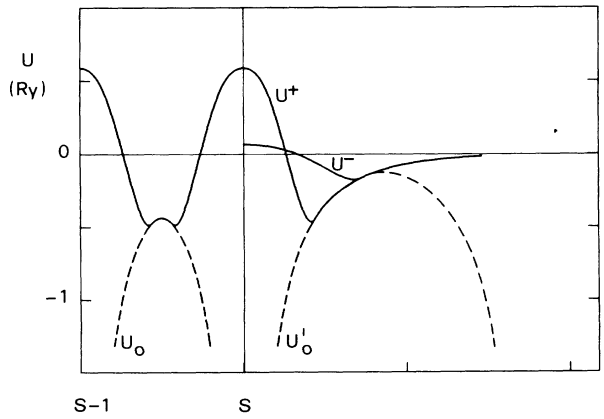


FIG. 8. One-dimensional nonlocal model potential constructed as explained in the text for symmetric ($U^+$) and antisymmetric ($U^-$) interlayer states, respectively. The broken lines represent the planar-averages $U_0$ and $U_0'$ of the self-consistent FLAPW potentials for the crystals with $c=c_0$ and $c=1.75c_0$, respectively. The vertical line indicates the location of the surface atomic plane.

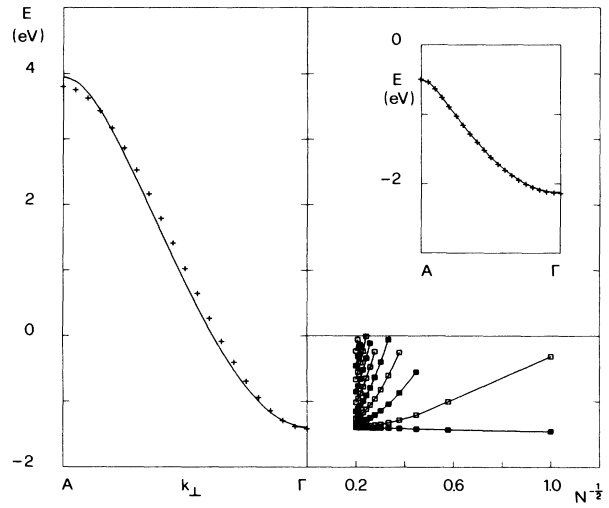


FIG. 9. Right panel: energies of bound states in $N$-layer model BN slabs with interlayer distance $c=c_0$. Even (odd) states are indicated by solid (open) squares. Left panel: lowest energy band for the infinite one-dimensional model BN crystal, compared with three-dimensional FLAPW band energies of interlayer states (crosses) calculated along the $\Gamma$-$A$ direction for the crystal with $c=c_0$. The same comparison for the crystal with $c=1.75c_0$ is given in the inset.

A weak ionic character results, however, from a small charge transfer towards the nitrogen atoms, in agreement with previous reports.[28] Figure 4 shows that the charge density is very weak in the interlayer region, even weaker than that predicted by the superposition of atomic densities (see Fig. 5). This reduction of electron density in the interlayer region is due to the formation of the strong bonds in the atomic planes.

More detailed information about the interlayer bonding is given in Figs. 6 and 7. In Fig. 6, we give the planar-averaged electron density calculated between two consecutive layers for a crystal with the equilibrium lattice parameter $c_0$ and for an expanded system with $c=1.75c_0$. For the latter system, the charge density at half distance between consecutive layers is practically zero. In this case, the atomic layers have essentially

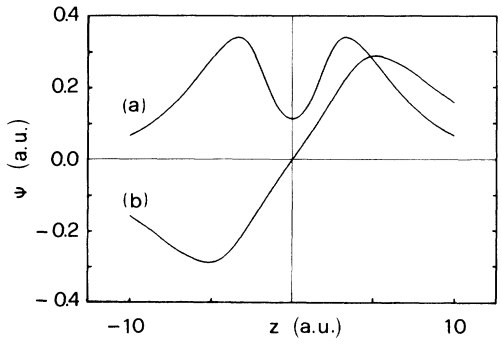


FIG. 10. Wave functions $\Psi$ of the symmetric (a) and antisymmetric (b) states bound to the isolated model BN monolayer. All values are in atomic units.

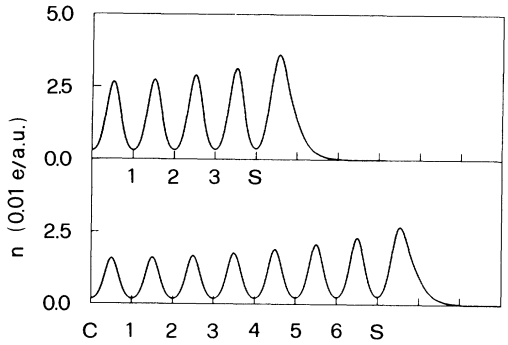


FIG. 11. Charge density of the ground state in a 9-layer (upper) and a 15-layer (lower) model BN slab, in units of 0.01 $e$/a.u. The surface layer is indicated by $S$ and the central layer by $C$.

nonoverlapping electron densities, and they can only interact through weak quadrupole or higher-order electrostatic forces. Figure 6 also shows that the charge density of the crystal with $c=c_0$ is well approximated by the superposition of charge densities of isolated layers, as obtained from the expanded system. The weak polarization effects occurring when the lattice spacing is reduced from $1.75c_0$ to the equilibrium value are shown in Fig. 7. In Fig. 7(a), we present a contour plot of the crystal density calculated for $c=c_0$ in the horizontal plane halfway from two consecutive layers. Polarization effects in the same horizontal plane are shown in Fig. 7(d), where we give the contour plot of the differential charge density, defined as the difference between the crystal density and the superposition of isolated-layer densities. This difference is positive everywhere in the plane, indicating that the layer-layer interaction enhances the interlayer charge density similarly to the situation occurring in the formation of a covalent bond. The polarization charge density, however, is only about 3% of the density itself, and has maxima in correspondence with facing atomic locations, and minima in correspondence with the centers of the hexagons. The enhancement of interlayer electron density due to polarization is not sufficient, however, to recover at the equilibrium interlayer distance the superposition of atomic densities in the interlayer region (see Fig. 5).

## V. MODEL CALCULATIONS FOR FINITE SLABS AND SURFACE PROPERTIES

We have extended the study of the electronic properties of $h$-BN by investigating its surface properties. Surface states which originate from bulk interlayer states have been found experimentally and theoretically in graphite.[24,25] Since our bulk band structure shows that interlayer band also exist in $h$-BN, we investigated the possible existence of surface states in this compound by performing one-dimensional model calculations on slabs with different thicknesses.

The results of the self-consistent FLAPW bulk calculations were used to construct a one-dimensional periodic model potential, in order to reproduce the $k_z$ disper-

sion of the interlayer bands. The electrostatic part $U_0$ of the model potential (including exchange and correlation contributions) is obtained as the $x$-$y$ planar average of the self-consistent FLAPW potential for the crystal with $c=c_0$. The total nonlocal model potential $U^{\pm}$ ($\pm$ referring to parity under $z$ reflection) is the sum of $U_0$ and a nonlocal orthogonality potential $U^{\pm}_{\rm orth}$ which has been obtained from FLAPW results for the expanded crystal ($c=1.75c_0$, which as shown previously, guarantees that the overlap between layer densities is negligible). The procedure followed in the derivation of $U^{\pm}_{\rm orth}$ contains four steps: (i) the FLAPW wave functions of the $\Gamma_1^+$ and $\Gamma_3^+$ interlayer states are averaged in the $x$-$y$ planes, and the resulting one-dimensional functions are made into pseudofunctions in correspondence with atomic planes, imposing continuity conditions and norm conservation;[29] (ii) these pseudofunctions are then introduced into a one-dimensional Schrödinger equation which is inverted, giving rise to a nonlocal norm-conserving total model potential for the expanded crystal; (iii) orthogonality potentials $U^{\pm}_{\rm orth}$ are then obtained by subtracting from the above model total potential the planar average $U_0'$ of the self-consistent FLAPW potential of the expanded crystal; (iv) we assume that the orthogonality potentials $U^{\pm}_{\rm orth}$ can be transferred to the crystal with $c=c_0$. The resulting potentials $U_0$, $U_0'$, and $U^{\pm}$ are displayed in Fig. 8. The soundness of our model is shown in Fig. 9, where we compare the results of the model for infinite one-dimensional periodic systems with FLAPW interlayer-band dispersion of the crystals with $c=c_0$ and $c=1.75c_0$.

In order to study surface properties, however, it is also necessary to extend the model potential into the vacuum region. This potential coincides with $U_0'$ close to the surface layer, and at large distances is approximated by the electrostatic potential (including exchange and correlation contributions) of an isolated layer. The Hartree term in the latter potential is obtained by $x$-$y$ planar averaging the Hartree potential resulting from the FLAPW calculation for the crystal with $c=1.75c_0$. The exchange and correlation contributions are calculated using the local-density approximation and a one-dimensional single-layer electron density which reproduces by superposition the $x$-$y$ planar average of the FLAPW density for the crystal with $c=1.75c_0$. The resulting potential in the vacuum region is displayed in Fig. 8.

This model has been used to study BN slabs with an odd number $N$ of layers ($1\leq N\leq 35$). The eigenvalues of bound states for these slabs are reported in Fig. 9. With increasing thickness, the energies converge towards the projected band structure of the infinite periodic system. Contrary to the case of graphite,[25] no surface state splits off at lower energy.

Further evidence that no surface state exists in $h$-BN is obtained by studying the evolution of the wave function of the ground state in slabs with increasing thickness. Two states, one symmetric (ground state), and one antisymmetric, are bound to the isolated monolayer. Their wave functions are displayed in Fig. 10. In Fig. 11, we give the charge density of the lowest bound state in the 9- and 15-layer slabs. We see in the sequence $N=1,9,15$ that the ground state becomes closer and closer to a Bloch state, and its amplitude does not decay appreciably inside the slab.

The absence of surface states in $h$-BN, despite its close similarity with graphite, can be related to the more pronounced atomic character that bulk interlayer states have in the former case. In fact, for graphite, the probabilities to be in the atomic spheres are 8% and 26% for the symmetric $\Gamma_1^+$ and the antisymmetric $\Gamma_3^+$ interlayer states, respectively, while the corresponding values for BN are 14% and 33% (1% and 0% in the boron sphere, 13% and 33% in the nitrogen sphere, respectively; the larger amount of charge in the nitrogen spheres is due to the greater electronegativity of this element compared with boron). Since bulk interlayer states in $h$-BN are more atomic in nature, they are less likely to give rise to surface states, which extend considerably into the vacuum region.

Finally, we notice that the model potential used in this work, being based on the LDA approximation, does not reproduce, far from the surface, the well-known image potential. Going beyond LDA and taking properly into account correlation effects, an infinite series of image states will result.[30]

## VI. CONCLUSIONS

We have presented a general study of the bulk and surface electronic properties of $h$-BN. We find that this material is an indirect-gap insulator, in contradiction with previous experimental and theoretical results. Furthermore, the conduction-band dispersion is complicated by the presence of two not-yet-reported bands, which correspond to empty interlayer states, and which are common to other layered materials. However, in contrast with the case of graphite, our LDA results do not show the existence of surface states originating from the interlayer bands.

## ACKNOWLEDGMENTS

The authors are grateful to Professor H. J. F. Jansen for close collaboration. This work was supported by the Swiss National Science Foundation and the U.S. National Science Foundation (Grant No. DMR 85-18607 and a computing grant from its Office for Advanced Scientific Computing at the University of Minnesota Computing Center). One of us (A.C.) acknowledges the financial support of the Consiglio Nazionale delle Ricerche (CNR), Italy.

*Present address: Istituto di Acustica O.M. Corbino, via Cassia 1216, I-00189 Roma, Italy.
†Also at Dipartimento di Fisica Teorica and GNSM-CNR, Università di Trieste, I-34014 Trieste, Italy.

[1]*Landolt-Börnstein: Numerical Data and Functional Relationships in Science and Technology*, edited by O. Madelung (Springer-Verlag, Berlin, 1982), Vol. 17a, p. 150.
[2]J. Zupan and D. Kolar, J. Phys. C **5**, 3097 (1972).
[3]W. Baronian, Mater. Res. Bull. **7**, 119 (1972).
[4]A. Zunger, A. Katzir, and A. Halperin, Phys. Rev. B **13**, 5560 (1976).
[5]M. J. Rand and J. F. Roberts, J. Electrochem. Soc. **115**, 423 (1968).
[6]R. Mamy, J. Thomas, G. Jezequel, and J. C. Lemonnier, J. Phys. (Paris) Lett. **42**, 473 (1981).
[7]D. M. Hoffman, G. L. Doll, and P. C. Ecklund, Phys. Rev. B **30**, 6051 (1984), and references therein.
[8]V. A. Fomichev, Fiz. Tverd. Tela (Leningrad) [Sov. Phys.—Solid State **13**, 754 (1971)]; V. A. Fomichev and M. A. Rumsh, J. Phys. Chem. Solids **29**, 1015 (1968).
[9]E. Tegeler, N. Kosuch, G. Wiech, and A. Faessler, Phys. Status Solidi B **84**, 561 (1977); E. Tegeler, N. Kosuch, G. Wiech, and A. Faessler, *ibid.* **91**, 223 (1979); J. Barth, C. Kunz, and T. M. Zimkina, Solid State Commun. **36**, 453 (1980).
[10]J. Cazaux, C. R. Acad. Sci. Ser. B **270**, 700 (1970).
[11]U. Büchner, Phys. Status Solidi B **81**, 227 (1977).
[12]R. D. Leapman and J. Silcox, Phys. Rev. Lett. **42**, 1361 (1979); R. D. Leapman, P. L. Fejes, and J. Silcox, Phys. Rev. B **28**, 2361 (1983).
[13]S. Larach and R. E. Shzader, Phys. Rev. **104**, 68 (1956).
[14]M. R. Vilanove, C. R. Acad. Sci. Ser. B **272**, 1066 (1972); **271**, 1101 (1970).
[15]R. Taylor, and C. A. Coulson, Proc. Phys. Soc. London, Sect. A **65**, 834 (1952).
[16]E. Doni and G. Pastori Parravicini, Nuovo Cimento B **64**, 117 (1969).
[17]A. Zunger, J. Phys. C **7**, 76 (1974); **7**, 96 (1974).
[18]R. Dovesi, C. Pisani, and C. Roetti, Int. J. Quantum. Chem. **17**, 517 (1980).
[19]J. Robertson, Phys. Rev. B **29**, 2131 (1984).
[20]J. Zupan, Phys. Rev. B **6**, 2477 (1972); J. Zupan and D. Kolar, J. Phys. C **5**, 3097 (1972).
[21]M. S. Nakhmanson and V. P. Smirnov, Fiz. Tverd. Tela (Leningrad) **13**, 3288 (1971) [Sov. Phys.—Solid State **13**, 2763 (1972)]; see also Fiz. Tverd. Tela (Leningrad) **13**, 905 (1971) [Sov. Phys.—Solid State **13**, 752 (1971)].
[22]A. Catellani, M. Posternak, A. Baldereschi, H. J. F. Jansen, and A. J. Freeman, Phys. Rev. B **32**, 6997 (1985).
[23]N.A. Holtzwarth, S. G. Louie, and S. Rabii, Phys. Rev. B **26**, 5382 (1982); M. Posternak, A. Baldereschi, A. J. Freeman, E. Wimmer, and M. Weinert, Phys. Rev. Lett. **50**, 761 (1983).
[24]Th. Fauster, F. J. Himpsel, J. E. Fisher, and E. W. Plummer, Phys. Rev. Lett. **51**, 430 (1983).
[25]M. Posternak, A. Baldereschi, A. J. Freeman, and E. Wimmer, Phys. Rev. Lett. **52**, 863 (1984).
[26]R. W. G. Wyckoff, *Crystal Structures* (Interscience, New York, 1965), Vol. 1; P. Villars and L. D. Calvert, *Pearson's Handbook of Crystallographic Data for Intermetallic Phases* (American Society for Metals, Metals Park, 1985), Vol. 2.
[27]H. J. F. Jansen and A. J. Freeman, Phys. Rev. B **30**, 561 (1984).
[28]J. C. Phillips, *Bonds and Bands in Semiconductors* (Academic, New York, 1973).
[29]G. B. Bachelet, D. R. Hamman, and M. Schlüter, Phys. Rev. B **26**, 4199 (1982).
[30]See, e.g., C. O. Almbladh and U. von Barth, Phys. Rev. B **31**, 3231 (1985); D. Straub and F. J. Himpsel, *ibid.* **33**, 2256 (1986).